

THE *EINSTEIN* GALACTIC PLANE SURVEY: STATISTICAL ANALYSIS OF THE COMPLETE X-RAY SAMPLEPAUL HERTZ¹ AND JONATHAN E. GRINDLAY²

Harvard-Smithsonian Center for Astrophysics

Received 1983 May 23; accepted 1983 August 15

ABSTRACT

A flux-limited survey of the galactic plane ($|b| < 15^\circ$) has been conducted using the Imaging Proportional Counter on board the *Einstein X-Ray Observatory*. The survey covered 275 deg^2 of the sky with a median limiting flux of $7 \times 10^{-13} \text{ ergs cm}^{-2} \text{ s}^{-1}$. Seventy-one unresolved serendipitous sources exceeding a 5σ threshold were detected.

A statistical analysis of the 71 sources indicates that $\sim 46\%$ of the sources are due to coronal emission from nondegenerate stars, $\sim 31\%$ are extragalactic in origin, and $\sim 23\%$ are neither coronal nor extragalactic. The last sources are presumably galactic accretion sources. The number-flux relation for low galactic latitude X-ray sources with $0.01 \lesssim f_x \lesssim 0.50 \text{ IPC counts s}^{-1}$ has a slope of -1.10 ± 0.16 ; this is significantly steeper than the slope of ~ -0.5 derived for the bright ($f_x \gtrsim 2 \text{ IPC counts s}^{-1}$) low-latitude X-ray sources detected by *Uhuru* and *Ariel V*. The X-ray sources detected in this survey are significantly concentrated toward the galactic center, both in galactic latitude and galactic longitude.

The number density and spatial distribution of the noncoronal, galactic fraction of the survey has been investigated in a statistical manner. High-luminosity neutron star binaries are inconsistent with the inferred mean luminosity for these sources. They are probably accreting white dwarfs, either low X-ray luminosity systems (e.g., cataclysmic variables at $\sim 10^{31-32} \text{ ergs s}^{-1}$) or moderate X-ray luminosity systems (e.g., the $\sim 10^{33-34} \text{ ergs s}^{-1}$ sources recently discovered in globular clusters by Hertz and Grindlay).

Subject headings: galaxies: Milky Way — galaxies: structure — luminosity function — stars: stellar statistics — X-rays: sources

I. INTRODUCTION

The *Einstein X-Ray Observatory* (*HEAO 2*; Giacconi *et al.* 1979a) is several orders of magnitude more sensitive than any other X-ray detector flown. In a typical (2–5 ks) exposure, sources with fluxes as small as $f_x \lesssim 0.02 \text{ IPC counts s}^{-1}$ may be detected with the Imaging Proportional Counter (IPC).³ This sensitivity allows us to study the nature of X-ray sources at distances significantly greater and luminosities significantly smaller than previous X-ray surveys (e.g., *Uhuru*, *Ariel V*, *HEAO 1*) have done. Since the *Einstein* mission consisted of pointed observations of previously selected astronomical objects and was not an all-sky survey, the most reasonable, statistically sound algorithm for conducting an unbiased study of the nature and distribution of low X-ray flux objects is to study the serendipitous sources detected in *Einstein* fields. In the *Einstein* Medium Survey, Maccacaro *et al.* (1982) investigated extragalactic X-ray sources by studying serendipitous sources found in *Einstein* fields at high galactic latitudes ($|b| > 20^\circ$). We shall investigate galactic X-ray sources by limiting our studies to serendipitous sources found in *Einstein* IPC fields at $|b| < 15^\circ$; we refer to our survey as the *Einstein* Galactic Plane Survey.

A medium sensitivity (as opposed to the Deep Surveys conducted with *Einstein*, e.g., Giacconi *et al.* 1979b and

Griffiths *et al.* 1983), flux-limited survey of the galactic plane may be used to investigate several interesting questions concerning the X-ray population of the Galaxy. The flux distribution of sources allows calculation of the number-flux relation [often referred to as the $\log(N > S) - \log(S)$ relation]. The slope of the number-flux relation gives important information on the spatial distribution of sources. The Galactic Plane Survey extends the flux limit of the *Uhuru* (Matilsky *et al.* 1973; Forman *et al.* 1978) and *Ariel V* (Warwick *et al.* 1981) number-flux relations by more than two orders of magnitude. This lower flux range is dominated by different classes of sources from the neutron star binaries which dominate the galactic plane at fluxes greater than $1 \text{ IPC count s}^{-1}$. The propensity of sources to be found in the galactic bulge as opposed to the galactic disk may be deduced from the longitude distribution of sources. In addition, the absolute number of sources observed at a given flux may be compared with that expected from known classes of galactic X-ray sources. An excess of new sources at low fluxes may indicate the presence of a new class of galactic X-ray sources; lack of an excess puts strong constraints on the existence of unknown classes of sources. Follow-up studies of individual sources will yield detailed information on single systems and may reveal peculiar new classes of objects.

We report here the *Einstein* Galactic Plane Survey. In § II we review the number-flux relations for bright galactic plane X-ray sources. § III contains a description of the detection algorithm employed in conducting the survey. We present the results of the survey in § IV. The implications of the survey are discussed in §§ V–VIII; we conclude in § IX.

¹ Currently at the E. O. Hulburt Center for Space Research, Naval Research Laboratory.

² Alfred P. Sloan Foundation Research Fellow.

³ $1 \text{ IPC count s}^{-1} \approx 2.3 \times 10^{-11} \text{ ergs cm}^{-2} \text{ s}^{-1}$ (0.15–4.5 keV) $\approx 1.0 \mu\text{Jy}$ averaged over Crab-like spectrum.

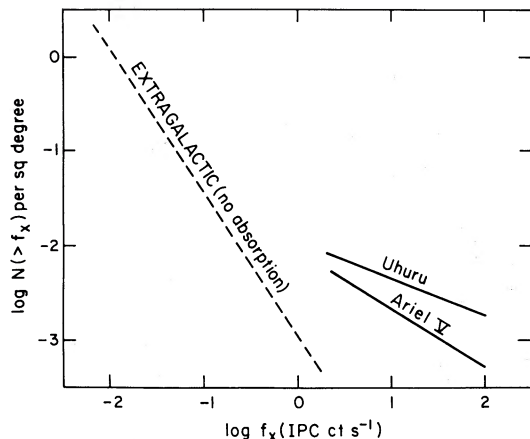


FIG. 1.—The number-flux relation for bright galactic X-ray sources and faint extragalactic X-ray sources. The $\log(N > S) - \log(S)$ curves plotted represent the low galactic latitude sources from the *Uhuru* 4U catalog (Forman *et al.* 1978) and the *Ariel V* 3A catalog (Warwick *et al.* 1981) as well as the extragalactic component of the *Einstein* Medium Survey (Maccacaro *et al.* 1982).

II. GENERAL NUMBER-FLUX RELATIONS

The 4U catalog (Forman *et al.* 1978) contains ~ 186 sources at low galactic latitudes ($|b| < 20^\circ$) detected by *Uhuru*. The derived number-flux relation is well fitted by the power law

$$N(>S) = 160S_U^{-0.4}, \quad (1)$$

where the flux S_U is in UFU.⁴ Assuming 1 UFU \approx 1 IPC count s^{-1} (Giacconi *et al.* 1979a) and normalizing the relation to sources per square degree yields

$$N(>f_x) = 1.1 \times 10^{-2} f_x^{-0.4} \quad (2)$$

for $2 \lesssim f_x \lesssim 100$, where f_x is the flux in IPC counts s^{-1} . Similar analysis of the 3A catalogue (Warwick *et al.* 1981), which contains 109 sources detected by *Ariel V* with $|b| < 10^\circ$, yields

$$N(>S_A) = 37S_A^{-0.62}; \quad (3)$$

here S_A is the source flux in *Ariel V* SSI counts s^{-1} .⁵ Using the approximate conversion 1 SSI count $s^{-1} \approx 2.3$ IPC counts s^{-1} (Warwick *et al.* 1981), and again normalizing to the number of sources per square degree yields

$$N(>f_x) = 0.87 \times 10^{-2} f_x^{-0.62} \quad (4)$$

for $2.3 \lesssim f_x \lesssim 230$; f_x is again in IPC counts s^{-1} .

In Figure 1 we have plotted the *Uhuru* and *Ariel V* number-flux relations for bright ($f_x \gtrsim 1$ IPC count s^{-1}) galactic plane X-ray sources. Given the approximations in converting the two sets of results to a common flux scale, the differing detector responses, and the different galactic latitudes included, the agreement is good. The most important result to note is that the slope of the galactic plane X-ray number-flux relation for bright sources is ~ -0.5 .

The slope of the number-flux relation describes the spatial distribution of the source population. Assume that there is a population of X-ray sources with a uniform space density ρ and normalized luminosity function $n(L)dL$ throughout a given

volume of space. If $V(L, S)$ is the volume in which sources of luminosity L may be observed with fluxes greater than S , then the number of sources (per 4π steradians) with fluxes exceeding S is

$$N(>S) = \int \rho V(L, S) n(L) dL. \quad (5)$$

Simple assumptions about the spatial distribution allow equation (5) to be integrated. For an isotropic distribution,

$$N(>S) = 0.094 \rho S^{-1.5} \langle L^{1.5} \rangle. \quad (6)$$

We have indicated by $\langle f(L) \rangle$ the average of a function of L weighted by the luminosity function $n(L)$, i.e., $\langle f(L) \rangle = \int f(L) n(L) dL$. For a two-dimensional, disk population

$$N(>S) = 0.5 \rho z S^{-1} \langle L \rangle, \quad (7)$$

where z is the scale height of the population. Finally, for a one-dimensional, linear population of sources

$$N(>S) = 0.56 \rho A S^{-0.5} \langle L^{0.5} \rangle. \quad (8)$$

Here A is the cross sectional area of the source population. Equations (6)–(8) show the canonical result of number-flux relations: they are power laws in S whose slope is independent of the luminosity function $n(L)$ and depends only on the spatial distribution of sources. One moment of the luminosity function determines the normalization of the number-flux relation.

The flat slope derived for bright ($f_x \gtrsim 2$ IPC counts s^{-1}) galactic plane X-ray sources may indicate that the sources have a primarily one-dimensional distribution; this is consistent with their lying along a spiral arm of the Galaxy (cf. Rothenflug, Rocchia, and Casse 1979). In Table 1 we show the approximate breakdown into various classes of the bright galactic sources from Bradt and McClintock (1983). Several classes, notably the massive X-ray binaries, are associated with the Population I stars of the spiral arms. However, massive binaries only account for $\sim 21\%$ of the ~ 115 bright sources. Johnson (1978) has pointed out that sources distributed uniformly throughout spiral arms with small pitch angles will exhibit a number-flux relation that is everywhere steeper than a slope of -0.5 . He argues that source variability may account for the flatness of the observed relation. Matilsky (1979) suggests that the flat slope

TABLE 1
CLASSES OF BRIGHT ($f_x \gtrsim 1$ IPC count s^{-1}) GALACTIC X-RAY SOURCES^a

Class of Sources	Number	Percent of Total
Massive neutron star binaries, e.g., SMC X-1, Cen X-3, X Per	24	21
Low mass neutron star binaries, e.g., Sco X-1, Her X-1, 4U 1735-44	33	29
Globular cluster sources, e.g., Rapid Burster, 4U 1820-30	9	8
Compact sources in supernova remnants, e.g., Crab Pulsar, SS 433	3	3
Cataclysmic variables, e.g., U Gem, AM Her, SS Cyg	10	9
Coronal emission sources, e.g., Algol, DM UMa	6	5
Unidentified sources (mostly galactic bulge) e.g., GX3+1, GX9+1	30	26

^a From Bradt and McClintock 1983.

⁴ 1 UFU $\approx 1.7 \times 10^{-11}$ ergs $cm^{-2} s^{-1}$ (2-6 keV).

⁵ 1 SSI count $s^{-1} \approx 5.3 \times 10^{-11}$ ergs $cm^{-2} s^{-1}$ (2-10 keV).

indicates most bright sources (excluding the galactic center sources) are situated in the solar neighborhood and, due to the Sun's position in the spiral arm, that the source density decreases with increasing distance. This is probably true for the coronal sources and the cataclysmic variables. These classes of sources make up $\sim 14\%$ of the bright sources. The flat slope of the number-flux relation for bright, low-latitude sources may also be explained by a nonuniform spatial distribution, presumably one increasing toward the galactic center (Protheroe and Wolfendale 1980). Certainly the mixture of many classes of X-ray sources with differing spatial distributions, luminosity functions, and variability time scales makes it difficult to unambiguously interpret the number-flux relation. The remaining bright sources are located in the galactic bulge (54%) and throughout the disk and halo ($\sim 11\%$). It is clear that rather complete optical identifications are necessary to thoroughly understand the number-flux relation.

As an aside, the high latitude number-flux relation for bright sources (Matilsky *et al.* 1973; Forman *et al.* 1978; McHardy *et al.* 1981), as well as the relation for the extragalactic component of X-ray sources with fluxes comparable to that studied in this work (Maccacaro *et al.* 1982) have slopes of ~ -1.5 . It is straightforward to interpret this in terms of a uniform population of X-ray sources throughout the universe. We have plotted the extragalactic number-flux relation from Maccacaro *et al.* (1982) in Figure 1.

The sensitivity of the *Einstein* Galactic Plane Survey is such that we have determined the number-flux relation for $0.01 \lesssim f_x \lesssim 0.5$ IPC counts s^{-1} . We can thus extend the galactic plane number-flux relation by ≥ 2 orders of magnitude. From these studies, we may determine the predominant population of X-ray sources at fluxes of ~ 0.02 – 0.1 IPC counts s^{-1} and compare these to the results for bright sources (e.g., see Table 1). From the high-latitude studies (Maccacaro *et al.* 1982) we know that there is a sizable extragalactic contamination of the survey. We take this into account explicitly when interpreting our results.

III. ANALYSIS OF X-RAY DATA

The *Einstein* Galactic Plane Survey was conducted with the IPC on board the *Einstein* X-Ray Observatory. Details of the instrumentation may be found in Giacconi *et al.* (1979a). In order to ensure that the survey is statistically complete and unbiased, we have carefully selected a set of IPC images for inclusion in the survey. These images were then searched for sources using an improved detection algorithm which corrects for the nonuniformity of the IPC detector. We briefly summarize our analysis procedure here; complete details may be found in Hertz (1983).

The Galactic Plane Survey fields were chosen from all IPC observations with targets located less than 15° from the galactic plane that were conducted by the Harvard-Smithsonian Center for Astrophysics, MIT Center for Space Research, Columbia Astrophysical Laboratory, and several guest observers (who kindly granted us permission to include their observations in the survey). The central $5'$ of each field of view were omitted from the survey to avoid sources associated with the target. Fields of view containing members of several classes of targets were excluded from the survey:

(i) sources known or expected to be extended in the IPC, e.g., supernova remnants, clusters of galaxies;

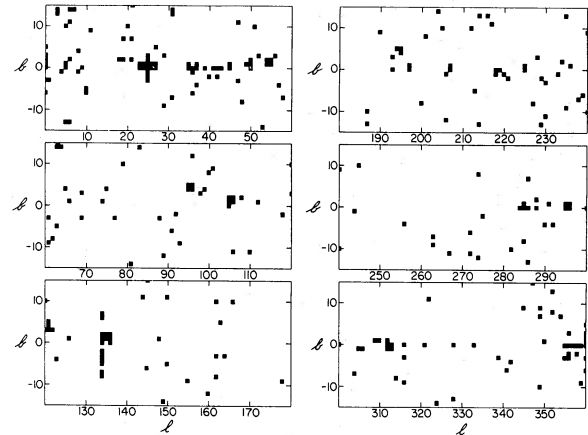


FIG. 2.—The distribution of fields for the *Einstein* Galactic Plane Survey. Each square represents the $1^\circ \times 1^\circ$ field of a single IPC observation. The 329 fields are shown plotted on a map of the galactic plane with $|b| < 15^\circ$.

(ii) sources which may contain several X-ray sources physically associated with the target (but located more than several arcminutes from it) thus making it difficult to identify sources as being serendipitous, e.g., OB associations, clusters of galaxies;

(iii) very bright classical X-ray sources which dominate the entire IPC field due to X-ray scattering from the telescope mirror, e.g., Cyg X-1.

All IPC fields included in the survey were inspected by eye for obvious problems (e.g., scattering from a nearby bright source or a large background flux from a diffuse source); all problem fields were excluded from the survey. The final survey contains 329 IPC fields covering 275.7 (2.6% of the galactic plane).

In Figure 2 we have plotted on a chart of the galactic plane each IPC observation included in the survey. A complete list of *Einstein* observations included in the Galactic Plane Survey may be found in Hertz (1983). The latitude and longitude distribution of observations in the survey is summarized in Table 2. As is evident, the coverage is fairly uniform (to a factor of ~ 4 in observations per square degree outside the

TABLE 2
DISTRIBUTION OF GALACTIC PLANE SURVEY FIELDS

Galactic Latitude (degrees) ^a	Number of IPC Fields	Fields per Square Degree
–15 to –11	20	0.012
–10 to –6	39	0.022
–5 to –2	41	0.028
–1 to 1	119	0.110
2 to 5	49	0.034
6 to 10	30	0.017
11 to 15	31	0.019
Galactic Longitude (degrees) ^a	Number of IPC Fields	Fields per Square Degree
–29 to 30	88	0.049
31 to 90	62	0.034
91 to 150	58	0.032
151 to 210	31	0.017
211 to 270	44	0.024
271 to 330	46	0.026

^a Coordinate of center of IPC field to the nearest degree.

galactic equator) and all portions of the galactic plane have been observed. Of course the observations are concentrated at low galactic latitudes and longitudes. Although the higher latitudes and longitudes are relatively undersampled, we shall see in § VIII that the coverage is sufficient to allow us to determine the dependence of source density on galactic latitude and longitude.

The input to the processing system is an IPC image file containing the position and PHA channel for each photon detected. The image is searched in three constant energy bands: soft (0.15–0.5 keV), hard (0.5–4.5 keV), and total (0.15–4.5 keV). In order to approximate constant energy bands, the PHA channels in each band have been adjusted according to the detector gain at the time of each observation.

Within each energy band, the image is searched for sources by looking for significant count excesses above the local background. The data in each energy band are binned into detection subcells where the size of each subcell is chosen to be ~ 0.5 FWHM of the mirror/detector point response function for that energy band. After study of the IPC point response function, we have chosen subcells of 12×12 pixels (soft), 6×6 pixels (hard), and 9×9 pixels (total) for the energy bands; one IPC pixel is $8''$. The source strength is taken from a 3×3 array of subcells centered on the source; the background is determined from a 1 subcell wide annulus surrounding the 3×3 detection array. We correct for the $\sim 15\%$ of the source photons which fall into the background region. We also correct for the effects of the detector window support ribs and the image mask at the edge of the field of view. We are thus able to use the entire 1 deg^2 field of view of the IPC.

Extensive Monte Carlo simulations have been carried out to determine the statistical reliability of the detection algorithm and the processing system. These simulations allow the statistical errors for a sample of sources to be calculated as a function of the survey detection threshold. For reasons discussed in § V, we have chosen a threshold of 5σ for the survey. We have also limited ourselves to sources unresolved by the IPC, i.e., sources with spatial extent less than $\sim 1'$, because the local detection algorithm fails for extended sources. With a threshold of 5σ , we expect < 0.3 spurious sources to be included in the survey results.

The positions of all X-ray sources detected were correlated with the *Einstein* Master Catalog for possible source identification. The Master Catalog is a compendium of 56 optical, radio, and X-ray catalogs which are disk resident on the *Einstein* computer. Objects from the Master Catalog which lie within $180''$ of a Galactic Plane Survey source are flagged as possible optical/radio identifications. Each is evaluated as a likely or unlikely candidate and the results are indicated in the final source catalog.

The error boxes for all Galactic Plane Survey sources were examined on the POSS prints and ESO plates. In addition, three color (*BVR*) CCD images for most northern ($\delta > -15^\circ$) sources in CFA fields were obtained at the 61 cm telescope of the Whipple Observatory (Hertz 1983). This "optical analysis" of the X-ray fields has two major purposes. The first is to identify possible optical counterparts for the sources discovered by the Galactic Plane Survey; optical identification of complete samples of galactic plane X-ray sources is currently in progress.

The second objective is to allow us to separate possible

coronal X-ray sources (i.e., coronal emission from non-degenerate stars) from accretion X-ray sources within our sample of sources. The *Einstein* Stellar Surveys (cf. Vaiana *et al.* 1981; Rosner *et al.* 1981; Helfand and Caillault 1982; Topka *et al.* 1982) indicate that all coronal sources have an X-ray to optical luminosity ratio of

$$\log(L_x/L_V) \lesssim -1.0; \quad (9)$$

the only exception may be dM stars (Vaiana *et al.* 1981; but see Helfand and Caillault 1982, and Hertz 1983). Thus any galactic point source with $\log(L_x/L_V) \gtrsim -1$ is not coronal and must be either an accretion source or extragalactic. Note, however, that some galactic accretion sources have $\log(L_x/L_V) \lesssim -1$, e.g., neutron stars with massive (e.g., Be) companions (cf. Rappaport and van den Heuvel 1982; Steiner *et al.* 1983). In addition, $\sim 35\%$ of known cataclysmic variables have $\log(L_x/L_V) \lesssim -1$ (Córdova and Mason 1983). We can only estimate the X-ray to optical luminosity ratio from the observed X-ray to optical flux ratio. However the dependence of f_x and f_V to reddening is similar for $A_V \lesssim 4$, so we assume $\log(L_x/L_V) \approx \log(f_x/f_V)$ (cf. Hertz 1983).

In order to determine a limit on $\log(L_x/L_V)$, the X-ray error circles have been searched for the brightest optical sources (stars) whose positions are consistent with that determined for the X-ray source. Whenever possible, we have used published magnitudes from bright star catalogs, e.g., SKYMAP (Gottlieb 1978) or magnitudes derived from our CCD observations (see Hertz 1983); otherwise the POSS prints and ESO plates were utilized. In order to estimate stellar magnitudes from the POSS/ESO plates, we calibrated the apparent diameter of stellar images on a 6X Polaroid enlargement of the plate with photometric magnitudes derived from 3 CCD observations (Hertz 1983) and two selected areas (Landolt 1973). We estimate that magnitudes determined from POSS/ESO plates are only accurate to ± 0.5 mag.

IV. RESULTS OF THE GALACTIC PLANE SURVEY

In Table 3 we present a catalog of sources detected by the Galactic Plane Survey. In this we have summarized information about each of the 71 5σ sources detected. The eight columns of the catalog contain the following information about each source:

Column (1): The 1E designation for the X-ray source.

Column (2): The right ascension (R.A.) and declination (decl.) of the X-ray source, to the nearest arcsecond, in 1950.0 coordinates. Note that this is the *Einstein* derived source location, even when a more accurate optical position is available.

Column (3): The galactic longitude (l) and galactic latitude (b) of the X-ray source, to the nearest $0^\circ 01'$.

Column (4): The radius, in arcseconds, of the 90% confidence limit error circle. Although the error radius depends on the source strength, its location in the field, and the energy band in which the source was detected, it is about $60''$ for the first IPC processing, $30''$ for reprocessed IPC images, and $3''$ – $5''$ for sources with HRI follow-up observations.

Column (5): The source flux (f_x) and 1σ uncertainty (δf_x) in the source flux. Both quantities are 0.15–4.5 keV fluxes in IPC counts s^{-1} .

Column (6): The signal-to-noise ratio (S/N) and the number of counts in the source above the local background (counts).

TABLE 3
X-RAY SOURCES FROM THE *EINSTEIN* GALACTIC PLANE SURVEY^a

Source Designation (1)	R.A. Decl. (2)	<i>l</i> <i>b</i> (3)	<i>r</i> (arcsec) (4)	f_x δf_x (5)	S/N counts (6)	<i>V</i> <i>X/O</i> (7)	Identification and Comments ^b (8)
1E 0206.3+5212	2 ^h 6 ^m 19 ^s .8 52°12' 32"	134.84 -8.61	24	0.267 0.015	17.5 473	14.9 0.2	CCD; Seyfert 1 (<i>z</i> = 0.05) (ref. 1) (variable in X-ray and optical)
1E 0236.6+6100	2 36 40.7 61 0 55	135.68 1.09	5	0.104 0.019	5.3 54	10.8 -2.1	LS I +61°303 = Be, radio star (ref. 2)
1E 0241.0+6215	2 41 1.1 62 15 30	135.64 2.43	5	0.402 0.013	30.0 1319	15.7 0.7	X0241+622 = QSO (<i>z</i> = 0.04) (ref. 3)
1E 0429.1+6432	4 29 8.6 64 32 33	144.06 11.35	57	0.038 0.006	6.7 73	8.0 -3.4	SAO 13185 = G0 V star
1E 0458.1+6529	4 58 8.9 65 29 50	145.27 14.33	24	0.301 0.017	17.5 431	>18.9 >1.8	CCD; (source spectrum cutoff)
1E 0540.0+4935	5 40 4.1 49 35 56	162.00 10.37	25	0.020 0.003	7.6 190	>15.5 >-0.7	CCD
1E 0548.0+0004	5 48 2.0 0 4 15	205.79 -13.46	28	0.037 0.007	5.3 79	14.8 -0.7	CCD; EG 289 = DA white dwarf (refs. 1 and 4)
1E 0627.4-1945	6 27 29.7 -19 45 55	228.49 -13.53	25	0.013 0.002	6.7 258	>17.2: >-0.2	
1E 0628.0-2010	6 28 4.3 -20 10 31	228.93 -13.57	24	0.028 0.002	11.9 470	>16.5: >-0.1	
1E 0629.2+0458	6 29 16.7 4 58 53	206.31 -2.07	56	0.029 0.005	6.3 119	6.8 -4.0	SAO 114010 = O6 star = Wackerling 1140 (ref. 5)
1E 0630.9+1748	6 30 59.2 17 48 33	195.13 4.27	5	0.124 0.006	20.9 773	>22.0 >2.5	2CG 195+04 = "Geminga" (ref. 6) (time variable; soft spectrum) (also $f_x = 0.118 \pm 0.011$)
1E 0634.4-2047	6 34 24.8 -20 47 44	230.15 -12.48	56	0.039 0.005	8.4 144	11.9: -1.9	G star (ref. 1)
1E 0643.0-1648	6 43 3.2 -16 48 28	227.38 -8.92	5	0.759 0.014	54.3 4239	13.2 -0.0	HL CMa = dwarf nova (ref. 7) (also $f_x = 0.462 \pm 0.016$) (also $f_x = 0.697 \pm 0.019$)
1E 0649.8-0515	6 49 53.9 -5 15 4	217.77 -2.22	29	0.047 0.008	6.1 66	6.3 -4.0	SAO 133807 = K0 star
1E 0655.6+2847	6 55 38.4 28 47 13	187.61 14.13	55	0.058 0.004	15.2 450	>11.3: >-1.9	(likely coronal source)
1E 0656.9+1418	6 56 58.0 14 18 31	201.11 8.26	5	0.335 0.019	17.3 605	>17.0: >1.1	
1E 0708.3-1713	7 8 21.3 -17 13 29	230.49 -3.71	58	0.075 0.013	5.9 58	8.9 -2.8	SAO 152506 = K0 III star
1E 0743.0+0346	7 43 1.6 3 46 9	215.88 13.72	26	0.035 0.004	7.9 154	11.7 -2.0	CCD; G star (ref. 1) (also $f_x = 0.016 \pm 0.004$) (also $f_x = 0.019 \pm 0.004$)
1E 0808.3-4725	8 8 19.5 -47 25 26	263.03 -7.76	55	0.184 0.015	12.7 253	>15.1: >0.1	(also $f_x < 0.010$) (source is transient/variable)
1E 0811.5-5704	8 11 30.4 -57 4 38	271.60 -12.49	57	0.083 0.015	5.4 92	>14.8: >-0.4	
1E 0830.3-2313	8 30 19.6 -23 13 24	245.59 9.65	26	0.031 0.004	7.1 132	>13.5: >-1.3	(likely coronal source)
1E 0830.9-2238	8 30 54.6 -22 38 27	245.19 10.10	27	0.016 0.003	6.6 120	>15.8: >-0.7	
1E 0843.1-5418	8 43 8.5 -54 18 36	271.89 -7.26	55	0.213 0.013	16.9 439	>16.2: >0.6	(source flares/variable)
1E 1021.5-5720	10 21 32.0 -57 20 29	284.11 -0.24	56	0.021 0.003	7.2 157	>14.0: >-1.3	(likely coronal source)
1E 1024.0-5732	10 24 5.8 -57 32 50	284.51 -0.23	55	0.073 0.005	16.4 503	12.8 -1.2	Wackerling 2134 (ref. 5) (also $f_x = 0.039 \pm 0.009$)
1E 1044.7-6400	10 44 42.0 -64 0 37	289.88 -4.61	30	0.036 0.007	5.4 63	5.2 -4.6	SAO 251117 = B8 star (binary stellar system; ref. 8)
1E 1145.0-6140	11 45 2.1 -61 40 31	295.49 -0.01	5	0.215 0.026	8.4 155	12.0 -1.1	X1145-616 = binary, pulsar = B1 I star (ref. 9)
1E 1145.5-6155	11 45 34.0 -61 55 39	295.61 -0.24	5	0.367 0.025	14.4 304	9.2 -2.0	SAO 251595 = B0 star X1145-619 = binary, pulsar (refs. 10 and 11)
1E 1218.7-6347	12 18 45.5 -63 47 11	299.67 -1.38	5	0.084 0.008	11.1 223	>12.4: >-1.3	Komeseroff 11 = radio source (ref. 12); young SNR candidate
1E 1220.8-6346	12 20 52.0 -63 46 36	299.90 -1.35	56	0.048 0.006	7.5 113	>15.4: >-0.3	
1E 1340.5-6107	13 40 30.1 -61 7 11	309.18 0.86	55	0.762 0.023	33.2 1617	8.4 -2.0	SAO 252429 = K0 III star (also $f_x = 0.276 \pm 0.035$) (source is variable)
1E 1414.4-6204	14 14 25.1 -62 4 39	312.82 -1.11	55	0.098 0.008	12.5 297	8.8 -2.7	SAO 252691 = G0 V star
1E 1449.7-6804	14 49 47.3 -68 4 12	313.94 -8.07	28	0.051 0.008	6.1 85	>16.5: >0.1	

TABLE 3—Continued

Source Designation (1)	R.A. Decl. (2)	<i>l</i> <i>b</i> (3)	<i>r</i> (arcsec) (4)	f_x δf_x (5)	S/N counts (6)	<i>V</i> <i>X/O</i> (7)	Identification and Comments ^b (8)
1E 1516.6–6826	15 16 39.9 –68 26 50	315.93 –9.63	57	0.014 0.003	5.3 86	> 15.4: > –0.9	
1E 1547.0–5410	15 47 3.5 –54 10 0	327.23 –0.14	58	0.045 0.008	5.3 63	> 14.8: > –0.6	Ref. (13)
1E 1616.5–5029	16 16 35.3 –50 29 55	333.04 –0.38	57	0.056 0.008	6.6 78	> 15.8: > –0.1	
1E 1618.8–5025	16 18 48.1 –50 25 22	333.34 –0.57	56	0.081 0.009	9.0 141	8.2 –3.0	SAO 243714 = F8 V star
1E 1624.5–3540	16 24 35.3 –35 40 22	344.65 9.01	58	0.119 0.021	5.6 53	9.3 –2.4	SAO 207684 = G0 V star
1E 1650.5–3020	16 50 33.2 –30 20 17	352.33 8.40	56	0.053 0.007	7.9 120	8.1 –3.2	SAO 208153 = A5 V star
1E 1715.9–4612	17 15 59.4 –46 12 21	342.67 –5.14	26	0.024 0.003	7.2 158	11.4 –2.3	Wackerling 3672 (ref. 5)
1E 1719.1–1946	17 19 7.4 –19 46 4	4.83 9.42	25	0.047 0.005	9.9 216	> 16.9: > 0.2	
1E 1731.4–3232	17 31 29.2 –32 32 12	355.68 0.05	56	0.129 0.012	10.6 206	5.7 –3.8	SAO 208977 = O7 binary star = Batten 486 (ref. 14)
1E 1739.3–2842	17 39 20.8 –28 42 34	359.82 0.69	56	0.102 0.012	8.2 112	9.1 –2.6	SAO 185635 = G5 IV star
1E 1740.7–2942	17 40 42.7 –29 42 46	359.12 –0.10	56	0.129 0.013	9.8 179	> 16.5: > 0.5	
1E 1742.9–2929	17 42 54.7 –29 29 58	359.56 –0.39	55	0.675 0.038	17.7 518	> 14.8: > 0.5	X1742–294 = GCX-1 (ref. 15)
1E 1746.7–3224	17 46 47.3 –32 24 52	357.50 –2.62	59	0.117 0.023	5.1 43	> 14.0: > –0.5	
1E 1747.9–2033	17 47 58.0 –20 33 12	7.80 3.28	24	0.169 0.017	9.9 307	> 13.0: > –0.8	CCD; (source flares/variable) (spectrum not cutoff)
1E 1751.1–2431	17 51 9.6 –24 31 44	4.76 0.61	58	0.055 0.010	5.7 61	> 13.0: > –1.3	(likely coronal source)
1E 1755.4+0427	17 55 28.2 4 27 57	30.81 13.93	25	0.082 0.009	9.3 168	11.0 –1.9	CCD; F–G star (ref. 1)
1E 1801.0–3018	18 1 2.8 –30 18 34	0.86 –4.19	57	0.068 0.010	7.1 94	> 10.0: > –2.4	(likely coronal source)
1E 1836.9–0724	18 36 56.8 –7 24 23	25.04 –0.75	57	0.018 0.003	5.4 75	8.9 –3.4	SAO 142475 = B3 star
1E 1847.4+3329	18 47 27.3 33 29 39	63.30 15.01	57	0.042 0.007	6.3 90	> 15.1: > –0.5	
1E 1848.1+3305	18 48 10.0 33 5 30	62.98 14.71	56	0.063 0.007	8.7 143	> 10.6: > –2.2	(likely coronal source)
1E 1851.6–3114	18 51 41.2 –31 14 24	4.93 –14.33	58	0.078 0.016	5.0 66	13.2 –1.0	V1223 Sgr = X1851–312 = cataclysmic variable (refs. 16 and 17)
1E 1854.0+0411	18 54 5.1 4 11 44	37.31 0.80	56	0.046 0.005	8.6 141	6.6 –3.9	SAO 124077 = G5 IV star
1E 1859.1+0122	18 59 8.0 1 22 52	35.39 –1.61	58	0.088 0.014	6.1 57	> 12.7: > –1.2	(likely coronal source)
1E 1912.3+1038	19 12 21.6 10 38 10	45.12 –0.22	29	0.018 0.003	5.3 67	9.7: –3.1	K star (ref. 1)
1E 1916.3–0009	19 16 18.8 –0 9 20	36.02 –6.13	26	0.029 0.004	7.4 129	> 14.5: > –0.9	
1E 1918.6+1857	19 18 39.8 18 57 45	53.18 2.36	27	0.057 0.009	6.4 101	> 13.5: > –1.0	
1E 1921.1+1501	19 21 6.9 15 1 30	49.99 –0.03	25	0.031 0.003	10.5 247	> 11.7: > –2.0	CCD; (likely coronal source) (source is variable) (spectrum is cutoff)
1E 1923.1+2010	19 23 10.8 20 10 40	54.76 2.00	28	0.020 0.004	5.3 90	6.3 –4.4	SAO 87186 = A1 V star
1E 1923.8+1405	19 23 50.3 14 5 39	49.49 –1.05	29	0.024 0.004	6.2 75	> 10.0: > –2.8	(likely coronal source)
1E 1928.1+1041	19 28 11.9 10 41 52	47.02 –3.62	55	0.036 0.004	9.8 250	> 15.8: > –0.3	
1E 1930.6+1101	19 30 38.9 11 1 22	47.60 –3.99	56	0.013 0.002	7.0 139	> 14.5: > –1.3	(likely coronal source)
1E 1948.1+0846	19 48 11.7 8 46 59	47.76 –8.85	5	0.008 0.002	5.1 75	8.0 –4.1	SKYMAP 19500128
1E 1948.8+0834	19 48 48.3 8 34 39	47.65 –9.08	5	0.080 0.004	19.6 659	> 8.6: > –2.9	(likely coronal source) (spectrum is soft and cutoff)

TABLE 3.—Continued

Source Designation (1)	R.A. Decl. (2)	l b (3)	r (arcsec) (4)	f_x δf_x (5)	S/N counts (6)	V X/O (7)	Identification and Comments ^b (8)
1E 2033.7+5935	20 33 44.6 59 35 39	95.39 11.46	27	0.009 0.002	5.1 104	>13.0: >-2.1	(likely coronal source)
1E 2035.5+6013	20 35 30.5 60 13 50	96.05 11.65	28	0.006 0.001	5.1 87	>9.4: >-3.6	(likely coronal source) (also $f_x = 0.009 \pm 0.003$)
1E 2141.2+4535	21 41 12.6 43 35 8	90.77 -6.99	5	0.033 0.006	5.1 50	>15.5 >-0.5	CCD
1E 2231.7+5622	22 31 45.8 56 22 14	104.81 -1.32	27	0.068 0.009	8.1 119	5.7 -4.1	SAO 34575 = K0 III star
1E 2331.6+4834	23 31 36.7 48 34 0	110.04 -12.08	57	0.031 0.005	6.2 84	>12.9 >-1.6	CCD; (likely coronal source)

^a See text for explanation of columns.

^b REFERENCES.—(1) Hertz 1983 and this work. (2) Bignami *et al.* 1981. (3) Appaparo *et al.* 1978. (4) Greenstein 1974. (5) Wackerling 1970. (6) Bignami, Caraveo, and Lamb 1983. (7) Chlebowski, Halpern, and Steiner 1981. (8) Gottlieb 1978. (9) Hutchings, Crampton, and Cowley 1981. (10) Lamb *et al.* 1980. (11) White *et al.* 1980. (12) Komeseroff 1965. (13) Lamb and Markert 1981. (14) Batten 1967. (15) Watson *et al.* 1981. (16) Reid *et al.* 1980. (17) Steiner *et al.* 1981.

The number of counts is merely an estimate; it is of course impossible to discriminate background counts from source counts.

Column (7): The V magnitude and X-ray to optical flux ratio $\log(f_x/f_V)(X/O)$. Where the source is unidentified, an upper limit on the optical flux and a lower limit on the flux ratio is derived from the brightest optical source within the 90% error circle. A colon (:) indicates that the magnitude is derived from our measurements of the POSS/ESO plates and is thus only good to ± 0.5 mag. Otherwise the V magnitude is from the referenced identification, the SKYMAP (Gottlieb 1978) or SAO (1966) catalogs, or our CCD observations (± 0.2 mag or better; Hertz 1983).

Column (8): Comments and miscellanea. We first indicate those sources for which we obtained CCD observations in three colors. We then report any optical or radio identification, with references. The flux observed in any other IPC observations is indicated by "also f_x ." Occasionally we indicate particularly interesting X-ray behavior for the brightest sources. References are given at the end of Table 3.

V. THE NUMBER-FLUX RELATION FOR THE GALACTIC PLANE SURVEY

In this section we construct the number-flux relation, i.e., the $\log(N > S) - \log(S)$ curve, for low-flux ($f_x \lesssim 1$ IPC count s^{-1}) galactic plane X-ray sources. Care must be taken to avoid systematic errors. The largest systematic error is due to the difference in the distribution of measured fluxes from the distribution of true fluxes. The slope of the number-flux relation constructed from the measured fluxes is systematically different from the slope of the true number-flux relation. By realizing that the slope is negative, we see that uncertainties in the flux will lead to more dim sources moving into a flux interval from below than bright sources moving in from above; presumably the same number of sources move out in both directions due to errors in the flux measurement. Thus the observed slope is systematically steeper than the true slope.

Murdoch, Crawford, and Jauncey (1973) have shown that the correction to the observed slope is relatively insensitive to the exact distribution of errors in the measurement of the fluxes for sources whose signal-to-noise ratio is $\gtrsim 5$. The correction may be calculated for less significant sources, but it

depends strongly on the error distribution for flux measurements. Since this is not known *a priori* and cannot be easily derived from the data, we have limited ourselves to the analysis of 5σ sources only. Marshall (1984) has pointed out that the correction factor derived by Murdoch, Crawford, and Jauncey (1973) is strictly valid only for surveys with a single flux limit. In the Galactic Plane Survey, each IPC field has a different distribution of flux limits. Since most sources are observed near threshold, and the fractional increase in the number of sources due to uncertainty in the flux is approximately the same for each IPC field, Marshall (1984) estimates that the actual correction to the observed slope is $\sim \frac{2}{3}$ of that calculated by the method of Murdoch, Crawford, and Jauncey (1973). In any case, the correction is small ($\lesssim 0.06$ in the slope) for our survey, and the uncertainty in the slope due to statistical errors dominates the correction term. Our interpretation of the Galactic Plane Survey is not dependent on the exact value of the slope of the number-flux relation.

In Figure 3 we present the sensitivity of the Galactic Plane Survey to 5σ sources. The sensitivity is determined by calculating the threshold for each subcell in the survey to a 5σ source. In Figure 3a we present a histogram of the threshold for the 689,253 subcells (275.7 deg^2) in the survey to 5σ sources. The fluxes are in IPC counts s^{-1} for the total (0.15–4.5 keV) band. We have integrated this distribution of thresholds to present the survey sensitivity in Figure 3b. Here we indicate the area surveyed as a function of limiting sensitivity.

The number-flux relation is straightforward to construct. For each source we note the area surveyed to that source's flux and the density of sources at that flux is then approximately one per area surveyed. Integrating this distribution yields the number-flux relation. In Figure 4 we present the number-flux relation for the 71 5σ sources in the Galactic Plane Survey. Note that the data graphed are extremely well approximated by a power law for $\log(f_x) \gtrsim -2.0$.

We have used the maximum-likelihood technique of Murdoch, Crawford, and Jauncey (1973) to determine the slope and normalization of the number-flux relation. We have chosen a minimum and maximum flux (S_{\min} , S_{\max}) between which to fit the relation and have also applied the correction to the slope so that the slope we quote is the slope for the distribution

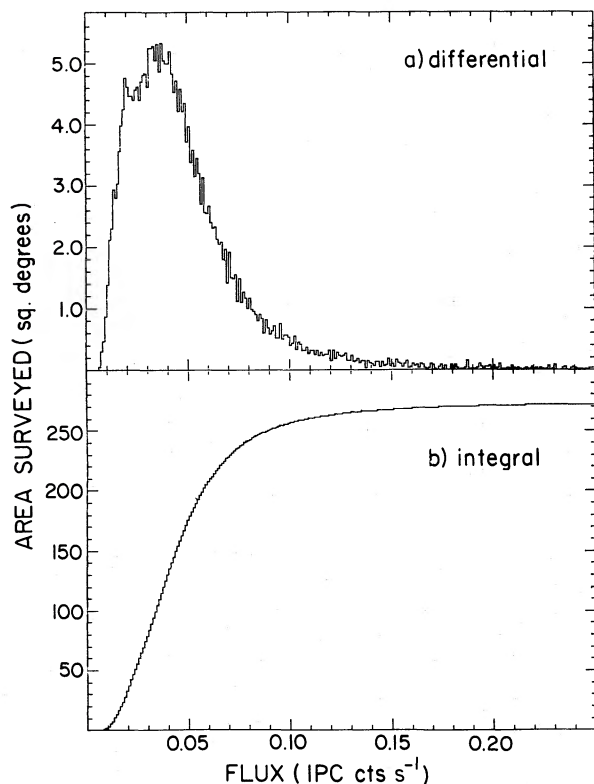


FIG. 3.—The sensitivity of the *Einstein* Galactic Plane Survey to 5σ sources. (a) The area surveyed as a function of limiting flux. The bin size for the flux is 0.001 IPC counts s^{-1} . (b) The area surveyed down to a limiting flux as a function of limiting flux. This is the integral of curve (a).

of true fluxes (i.e., the correction factor of Murdoch, Crawford, and Jauncey 1973 has been applied), not the slope of the distribution of measured fluxes plotted in Figure 4. We find that

$$N(>f_x) = 5.0 \times 10^{-3} f_x^{-(1.10 \pm 0.16)} \quad (10)$$

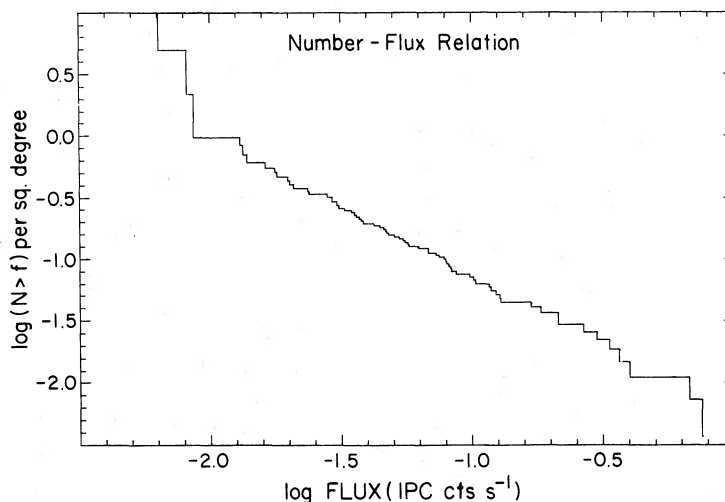


FIG. 4.—The number-flux relation for low galactic latitude X-ray sources. This is the distribution of the observed fluxes for the 71 5σ sources detected in the *Einstein* Galactic Plane Survey. We have plotted the number of sources per square degree with fluxes exceeding f_x as a function of f_x in IPC counts s^{-1} .

for faint galactic plane X-ray sources,⁶ this relation has been determined for $0.01 \lesssim f_x \lesssim 0.50$ IPC counts s^{-1} .

We have plotted this result, along with the *Uhuru* (Forman *et al.* 1978) and *Ariel V* (Warwick *et al.* 1981) results in Figure 5. We note, reassuringly, that the number-flux relation is apparently continuous from very high fluxes ($f_x \gtrsim 100$ IPC counts s^{-1}) to very low fluxes ($f_x \lesssim 0.01$ IPC counts s^{-1}). The number-flux relation for low latitude X-ray sources is now known over approximately four orders of magnitude in the X-ray flux. Note that the relation steepens considerably around ~ 1 IPC counts from a slope of ~ -0.5 to a slope of ~ -1.1 . This is not unexpected. At high fluxes the majority of sources are galactic accretion sources (see Table 1) which appear to have an approximately linear spatial distribution. The slope is thus flatter at high fluxes. As we include lower fluxes in our survey, we become more sensitive to two classes of X-ray sources which are absent (or poorly represented) at high fluxes: coronal sources (i.e., X-rays from nondegenerate stars) and extragalactic sources (e.g., AGNs and clusters of galaxies). The Medium Survey found that essentially all high latitude faint sources fall into the latter two categories (Stocke *et al.* 1983). Extragalactic X-ray sources are distributed isotropically, i.e., their number-flux relation has slope -1.5 (Maccacaro *et al.* 1982). The coronal sources detected are primarily nearby stars (Vaiana *et al.* 1981) so that the detection distance is typically less than the scale height of the stars in each stellar population and are thus apparently distributed isotropically. Inclusion of these sources will significantly steepen the slope of the number-flux relation. We observe this occurring in Figure 5.

VI. CONTRIBUTIONS TO THE GALACTIC PLANE SURVEY

At this point we estimate what fraction of the 71 5σ sources in the Galactic Plane Survey are coronal, extragalactic, or galactic accretion sources. We may predict the extragalactic fraction quite straightforwardly. We know from the Medium

⁶ Here, and throughout our discussion of number-flux relations, f_x is in IPC counts s^{-1} and $N(>f_x)$ is in sources per deg^2 .

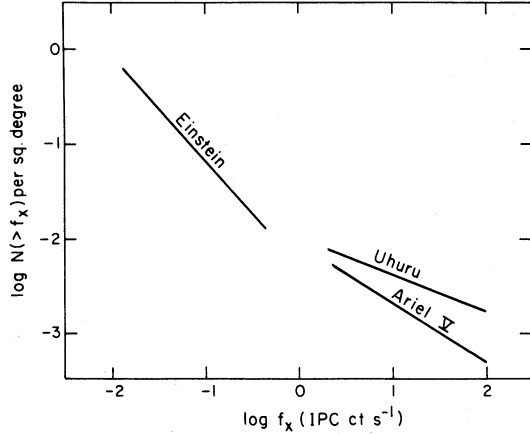


FIG. 5.—The number-flux relations for three surveys of the galactic plane. The *Uhuru* and *Ariel V* surveys are the same as in Fig. 1. The *Einstein* result represents the maximum likelihood fit to the distribution of observed fluxes shown in Fig. 4. Note that the overall number-flux relation is continuous (as required) and that it steepens near fluxes of ~ 1 IPC counts s^{-1} .

Survey (Maccacaro *et al.* 1982) that the distribution of extragalactic X-ray sources is isotropic, and that the number-flux relation is

$$N(> f_x) = 1.1 \times 10^{-3} f_x^{-1.52} \quad (11)$$

for extragalactic sources. We must fold this distribution through the parameters of our survey taking into account two effects: extinction in the galactic plane, and the varying sensitivity of the 329 observations in our survey. We assume that the galactic extinction may be approximated by a cosecant reddening law, i.e.,

$$N_H \approx 4.1 \times 10^{20} \csc(|b|) \quad (12)$$

(Allen 1973; Gorenstein 1975). We fit an approximate conversion from N_H to E_a (X-ray spectral cutoff energy)

$$\log(N_H) \approx 21.8 + 2.48 \log(E_a) \quad (13)$$

(Zombeck 1980) so that equation (12) becomes

$$E_a \approx 0.28 [\csc(|b|)]^{0.4}. \quad (14)$$

We also fit the sensitivity of the IPC to E_a for a power-law spectrum with spectral index 0.4 (Giacconi *et al.* 1978) and obtain

$$f_x(E_a) \approx 1.35 \cdot 10^{-0.42 E_a f_x} (E_a = 0.3); \quad (15)$$

we have normalized the relation to $E_a = 0.3$ keV and used a spectral index of 0.4 since this is the X-ray spectrum assumed by the Medium Survey in determining the extragalactic number-flux relation. Finally we note that the varying sensitivities of the survey fields have already been calculated (cf. Fig. 3). The expected number of extragalactic sources is therefore

$$N_{eg} \approx \int df_x \int db \frac{dN(> f_x)}{df_x} A[r(b)f_x], \quad (16)$$

where

$$r(b) = 1.35 \cdot 10^{-0.42 E_a(b)}, \quad (17)$$

$E_a(b)$ is given by equation (14), $A(rf_x)$ is the area in the survey with limiting sensitivity greater than rf_x , and the integration is over all survey fields. The result of this calculation is that we expect ~ 22.0 extragalactic sources out of the 71 5σ sources.

Next we wish to estimate the number of coronal sources in the survey. It is easier to estimate the number of noncoronal (i.e., galactic accretion and extragalactic) sources, so we simply estimate the number of noncoronal sources and accept the remainder of the total as coronal sources. We assume that all coronal sources have $\log(f_x/f_V) \lesssim -1$ and that all noncoronal sources have $\log(f_x/f_V) \gtrsim -1$. This is an excellent assumption for a sample of serendipitous X-ray sources (Stocke *et al.* 1983), although it is conservative for accretion sources since massive X-ray binaries (e.g., Be stars) and some cataclysmic variables will not satisfy this criterion. First we collect all sources for which the brightest star in the error box is so faint that $\log(f_x/f_V) \gtrsim -1$. Since the dependence of f_x and f_V to reddening is similar for $A_V \lesssim 4$, we ignore reddening effects to the first order. (At larger A_V , which could be expected only for $|b| \lesssim 2.5$ on the basis of the cosecant reddening law, the ratio f_x/f_V is larger than the ratio of luminosities L_x/L_V .) There are 30 sources for which $\log(f_x/f_V) \gtrsim -1$; these are probably noncoronal. We next calculate the probability that a noncoronal source will be projected near a bright ($V \lesssim 15$) star on the sky and thus tentatively classified as coronal; this probability is a function of the X-ray flux. For a given flux f_x , the probability that a noncoronal source will be tagged as coronal is the probability that a star with V such that $\log(f_x/f_V) < -1$, or

$$V < 2.5[-1 - \log(f_x) + 5.2], \quad (18)$$

will be found in the IPC error box. If N_V is the surface density of stars brighter than V , then the probability desired is

$$p = 1 - \exp(-N_V a_\sigma), \quad (19)$$

where a_σ is the area of an IPC error circle (~ 3 arcmin²). Tables of N_V as a function of galactic latitude (Allen 1973) allow us to calculate the probability as

$$p(f_x) = \int db \{1 - \exp[-N_V(f_x) a_\sigma]\} A(b)/A_{tot}, \quad (20)$$

where $A(b)$ is the area surveyed to limiting flux f_x at latitude b , A_{tot} is the total area surveyed to limiting flux f_x , $N_V(f_x)$ for calculating N_V is given by equation (18), and the integral is again over all survey fields. We calculated $p(f_x)$ for several fluxes and fitted a smooth curve to it,

$$\log[p(f_x)] = -2.00 - 1.21 \log(f_x) - 0.16[\log(f_x)]^2. \quad (21)$$

We then determined the corrected number of noncoronal sources in the survey as

$$N_{nc} = \sum [1 - p(f_x)]^{-1}, \quad (22)$$

where the summation is over the fluxes of the 30 sources which are probably noncoronal. This yields an estimate of 38.3 noncoronal sources in the sample of 71 5σ sources. Combining our two estimates yields ~ 32.7 (46%) coronal sources, ~ 22.0 (31%) extragalactic sources, and ~ 16.3 (23%) galactic accretion sources (see Table 4). The approximate uncertainty in these fractions is $\approx 5\%$ and is due to both statistical

TABLE 4
EXPECTED SOURCE FRACTIONS FOR GALACTIC
PLANE SURVEY

Type	Number	Fraction
Coronal	32.7	46%
Extragalactic	22.0	31%
Galactic accretion	16.3	23%

uncertainties and the approximations made in estimating various parameters.

VII. THE LOW-FLUX GALACTIC ACCRETION SOURCES

We have plotted the number-flux relations for subsets of the data in Figure 6. In Figure 6a we plot the number-flux relation for the 30 noncoronal sources corrected by the probability of false coronal identifications given by equation (21). In Figure 6b we give the predicted relationship for extragalactic sources from the derivative of equation (16). We give the difference of Figures 6a and 6b in Figure 6c. Presumably this is the number-flux relation for faint galactic

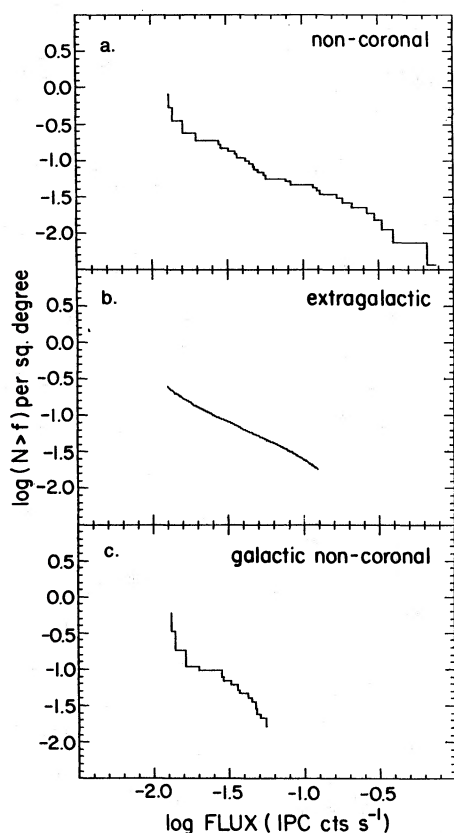


FIG. 6.—The number-flux relations for several subsets of the *Einstein* Galactic Plane Survey. (a) The number-flux relation for the 30 noncoronal [i.e., $\log(f_x/f_V) \geq -1$] sources in the survey corrected by the probability of a noncoronal source being superposed near a bright star. (b) The predicted number-flux relation for extragalactic X-ray sources in the Galactic Plane Survey. The curve is poorly known for large fluxes (no sources) and for small fluxes (no area surveyed). (c) The difference of (a) and (b), which presumably is the number-flux relation for noncoronal galactic X-ray sources.

accretion sources. In practice, although our estimates of the integrated numbers of sources in each class are likely to be correct, the calculations have too many approximations for the number-flux estimates to be accurate. Determination of the number-flux relations for various classes of galactic plane X-ray sources will have to await a complete sample of optically identified sources.

We can, however, use the information in Figure 6c to investigate the possible classes of galactic X-ray sources which contribute to the 23% of the sources in our survey which we have classified as galactic accretion sources. We expect faint galactic accretion sources to lie within the disk of the Galaxy and thus to have a slope of -1 in the number-flux relation. A formal fit to Figure 6c yields a slope of ~ -1.2 ; given all of the uncertainties in estimating the number-flux relation for galactic accretion sources as well as the small number of sources, we consider this to be a reasonable agreement with the expected slope of -1 . Assuming a slope of -1 , the number-flux relation for galactic accretion sources has an approximate normalization of 2.2×10^{-3} sources per square degree with $f_x > 1$ IPC count s^{-1} . Thus we assume that the number-flux relation is given by

$$N(> f_x) = 2.2 \times 10^{-3} f_x^{-1} \quad (23)$$

for faint galactic accretion sources.

By comparing equation (23) to equation (7), we have

$$\rho z \langle L_x \rangle = 4.0 \times 10^{28}, \quad (24)$$

where ρ is the space density of sources in pc^{-3} , z is their scale height in pc, and $\langle L_x \rangle$ is the mean X-ray luminosity of the sources in $ergs\ s^{-1}$. In Figure 7 we have plotted equation (24) for 3 values of z which bracket all conceivable scale heights. Note that due to the large dynamic range in the scales of Figure 7, the choice of z is not critical. This figure tells us that a population of sources which dominates the 23% of the galactic plane sources which we have categorized as galactic accretion sources must have $(\rho, \langle L_x \rangle)$ lying on the locus plotted. Consider several possible classes of galactic accretion sources:

(i) *Low-mass neutron star binaries* have $\langle L_x \rangle \simeq 10^{37}-10^{38}$ $ergs\ s^{-1}$ (Bradt and McClintock 1983). The spatial density of low-mass neutron star binaries is $\rho \sim 5 \times 10^{-10}$ pc^{-3} (Patterson 1983). We have plotted these data in Figure 7. Note however that all neutron star binaries with $L_x \geq 10^{36}$ $ergs\ s^{-1}$ are located within 30 kpc and have $f_x \geq 1$ IPC count s^{-1} . Thus low-mass neutron star binaries are eliminated as possible contributors to the low flux accretion sources identified in the Galactic Plane Survey.

(ii) *Massive X-ray binaries* usually have $L_x \geq 10^{36}$ $ergs\ s^{-1}$ (Bradt and McClintock 1983) and thus also have $f_x \geq 1$ IPC count s^{-1} . The few Be star-neutron star binaries which have $L_x \lesssim 10^{36}$ $ergs\ s^{-1}$ generally have $\log(f_x/f_V) \lesssim -1$ (Rappaport and van den Heuvel 1982). In either case, the low-flux accretion sources cannot be massive X-ray binaries.

(iii) *White dwarf binaries* have recently been discovered in globular clusters (Hertz and Grindlay 1983a). These sources are several orders of magnitude more luminous than cataclysmic variables and may represent a separate class of X-ray source. If the luminosity function of white dwarf binaries

is the same in the galactic plane as it is in globular clusters⁷ then it has a slope of ~ 1.2 and a maximum of $\sim 10^{34.5}$ ergs s^{-1} (Hertz and Grindlay 1983a, b); thus $\langle L_x \rangle \approx 10^{34}$ ergs s^{-1} . We have no way of measuring the density in the galactic plane. If we assume that the ratio of white dwarf binaries to neutron star binaries is the same in the galactic plane as it is in globular clusters, i.e., ~ 200 to 1 (Hertz and Grindlay 1983a), then $\rho \approx 2 \times 10^{-7}$ pc $^{-3}$. This is plotted in Figure 7.

(iv) *Cataclysmic variables* are also white dwarf binaries, but we have noted that they typically have lower X-ray luminosities than the dim globular cluster X-ray sources. They may, however, be the two ends of a single distribution of sources (Hertz and Grindlay 1983a; see below). The cataclysmic variables have a relatively well-determined mean luminosity $\langle L_x \rangle \approx 10^{31.5 \pm 0.7}$ ergs s^{-1} (Córdova and Mason 1983) and spatial density $\rho \approx 6 \times 10^{-6}$ pc $^{-3}$ (Patterson 1983); these values are plotted in Figure 7.

(v) *Coronal sources* have also been plotted in Figure 7 for comparison. They are not considered as a possible identification for the faint galactic accretion sources because they have previously been eliminated on the basis of their X-ray to optical flux ratio; in addition they have a locally isotropic distribution. We have taken the stellar densities from Allen (1973) and the mean X-ray luminosities for dF stars from Topka *et al.* (1982) and for dM stars from Rosner *et al.* (1981). The data for RS CVn stars are from Walter (1981).

All of the source classes discussed lie on or near the locus of sources detected by the Galactic Plane Survey and classified as noncoronal galactic sources. The coronal sources (dF stars, dM stars, RS CVn stars) were eliminated on the basis of their

X-ray to optical flux ratios. We have eliminated the neutron star binaries because the low fluxes for the unidentified serendipitous sources ($f_x \lesssim 0.1$ IPC count s^{-1}) are inconsistent with the high luminosities of neutron star binaries ($L_x \gtrsim 10^{36}$ ergs s^{-1}) and a galactic origin.

This leaves two classes of sources which have a combination of spatial density and mean luminosity which is consistent with the number-flux relation derived for noncoronal galactic sources (what we have referred to as faint galactic accretion sources above). The luminous white dwarf binaries and the less luminous cataclysmic variables are similar in that they are both presumed to be white dwarfs with accreting low mass secondaries. Hertz and Grindlay (1983a) have already noted that the luminosity function of the dim globular cluster X-ray sources, identified with white dwarf binaries, and that of the cataclysmic variables are consistent. They determined the slope of the luminosity function to be ~ -1.2 (see Fig. 2 of Hertz and Grindlay 1983b). A luminosity function is a relationship between ρ and L_x , as is equation (24). Since the slope of the luminosity function for white dwarf binaries is ~ -1 , this ensures that sampling the luminosity function at different luminosities and deriving the respective densities at these luminosities will generate points which lie on the locus plotted in Figure 7.

We thus conclude that the majority of the noncoronal galactic sources in the Galactic Plane Survey are white dwarfs with accreting low-mass companions. We identify this class of source with cataclysmic variables, which have a different X-ray luminosity and are, in general, optically selected. The location of both the high- and low-luminosity ends of the luminosity function on the locus defined by the Galactic Plane Survey confirms that the slope of the luminosity function is ~ -1 , as derived by Hertz and Grindlay (1983b). We infer from Figure 7 that the spatial density of these sources is $\sim 3 \times 10^{-7}$ pc $^{-3}$ for high-luminosity sources ($L_x \approx 10^{34}$ ergs s^{-1}) and $\sim 3 \times 10^{-5}$ pc $^{-3}$ for low-luminosity sources ($L_x \approx 3 \times 10^{31}$ ergs s^{-1}).

⁷ This may not be a good assumption. White dwarf binaries presumably form via the two-body tidal interaction in globular clusters (Hertz and Grindlay 1983a) whereas they may evolve from initial binaries in the galactic plane (Patterson 1983). There is no reason why the luminosity function for two populations with different evolutionary schemes should be the same, in spite of the physical similarities of the systems.

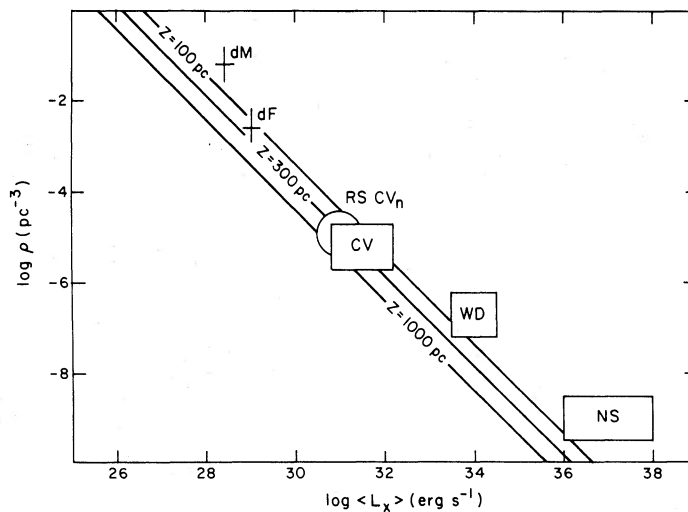


FIG. 7.—The locus of noncoronal galactic X-ray sources in the (ρ, L_x) plane. The three straight lines represent the required locations on the (ρ, L_x) plane of noncoronal galactic X-ray sources for three assumed values of the source distributions scale height ($z = 100$ pc, $z = 300$ pc, $z = 1000$ pc). The figures plotted represent different populations of galactic X-ray sources: dM stars (dM), dF stars (dF), RS CVn stars (RS CVn), cataclysmic variables (CV), accreting white dwarfs (WD), and neutron star binaries (NS).

VIII. CONCENTRATION OF SOURCES IN THE GALACTIC BULGE

Now that we have a hypothesis about the nature of the dim galactic accretion sources in our survey, we examine the survey results to determine if there is any dependence on galactic latitude and longitude in the distribution of serendipitous galactic plane X-ray sources. We have divided the sample into several latitude and longitude bands. For each band we have derived the number-flux relation and fitted the maximum likelihood (Murdoch *et al.* 1973) power-law slope and normalization. In Table 5 we report the results of this exercise. For each cut in the survey we report the number of 5σ sources included in the cut, the minimum and maximum fluxes for fitting the number-flux relation,⁸ the number of sources included in the fit, and the (corrected) maximum likelihood slope and normalization. Note that for the normalization we quote the density of source per square degree brighter than 0.1 IPC count s^{-1} .

Both the latitude and longitude cuts reveal correlation between the coordinates of the surveyed region and the normalization and slope of the number-flux relation. Sources are concentrated toward low galactic latitudes and longitudes. Sources brighter than 0.1 IPC count s^{-1} are found to be ~ 6 times more numerous toward the galactic center than toward the galactic anticenter. The brighter of these sources have $L_x \approx 2 \times 10^{34}$ ergs s^{-1} , consistent with the most luminous accreting white dwarfs found in globular clusters (Hertz and Grindlay 1983a, b) if they are indeed at $d \sim 10$ kpc. Similarly the source density is $\sim 50\%$ higher at low latitudes ($|b| < 2.5^\circ$) than at medium latitudes ($5^\circ < |b| < 15^\circ$). Testing the linear correlation coefficient between the mean latitude or longitude and the number of sources brighter than 0.1 IPC count s^{-1} (K in Table 5) shows significant correlation (95% confidence level) between source density and mean longitude and marginal correlation (82% confidence level) between source density and mean latitude.

We also note that the slope of the number-flux relation changes systematically with galactic latitude and longitude; it is flatter toward the galactic center and steeper away from it. In both cases the correlation is significant (98% confidence level for longitude, 92% confidence level for latitude) even when the rather large uncertainties in the slope α are taken into account. This is understandable because we expect galactic sources to dominate near the galactic center and extragalactic

⁸ We have fitted that part of the number-flux relation which is well approximated by a power law.

sources, with their steeper slope, to be a significant contribution at high latitudes and toward the galactic anticenter. Note also that the sources at low latitudes appear to be distributed with a slope significantly flatter than -1 . This implies that there may be a larger concentration of galactic accretion sources, presumably the accreting white dwarfs discussed in the previous section, with a distribution similar to that of the bright sources ($f_x \gtrsim 1$ IPC count s^{-1}) in the galactic bulge. Optical identifications will allow us to confirm this hypothesis directly.

IX. CONCLUSIONS

We have conducted a flux-limited survey of the galactic plane ($|b| < 15^\circ$) using the *Einstein* IPC. We have surveyed 275.7 deg^2 to a mean flux limit of ~ 0.03 IPC count s^{-1} and discovered 71 pointlike X-ray sources exceeding a 5σ threshold. Optical identification of complete samples of galactic plane X-ray sources is in progress.

We have analyzed statistically the 71 5σ sources and drawn the following conclusions:

(i) The number-flux relation for low-flux galactic plane X-ray sources has a slope of -1.10 . This is significantly steeper than the slope of ~ -0.5 determined for bright galactic plane X-ray sources by *Uhuru* and *Ariel V*. The steepening is due to the different source population at low fluxes (e.g., AGNs and nondegenerate stars) than at high fluxes (e.g., accreting neutron stars).

(ii) The sample contains $\sim 46\%$ coronal sources, $\sim 31\%$ extragalactic sources, and $\sim 23\%$ galactic accretion sources. This means we have discovered ~ 16 new galactic accretion sources. Optical identification of the sources and studies of individual systems will increase our understanding of low flux galactic accretion sources.

(iii) The approximate number density of the galactic accretion source subset of the survey is consistent with these sources being cataclysmic variables and other accreting white dwarfs. If this is the case, then we will discover a sizable number of X-ray selected cataclysmic variables. This will have implications on the total number density of cataclysmic variables as well as their X-ray luminosity function (Patterson 1983).

(iv) Faint galactic plane sources are significantly concentrated toward the galactic bulge. In addition, sources near the bulge exhibit a flatter number-flux relation than those at higher galactic latitudes and longitudes. This indicates a different source population with a less isotropic distribution.

TABLE 5
NUMBER-FLUX RELATIONS FOR THE GALACTIC PLANE SURVEY

Sources	N_{tot}	S_{min}	S_{max}	N_{fit}	α	K^a
All.....	71	0.013	0.45	65	1.10 ± 0.16	6.3×10^{-2}
$ b > 5^\circ$	32	0.015	0.30	24	1.15 ± 0.29	4.4×10^{-2}
$ b < 2.5^\circ$	29	0.020	0.50	24	0.92 ± 0.27	6.9×10^{-2}
$b > 2.5^\circ$	18	0.015	0.30	14	1.09 ± 0.38	3.9×10^{-2}
$b < -2.5^\circ$	24	0.015	0.25	18	1.08 ± 0.35	5.8×10^{-2}
$ l < 30^\circ$	16	0.015	0.30	15	0.64 ± 0.36	11.5×10^{-2}
$30^\circ < l < 110^\circ$	20	0.010	0.07	14	0.99 ± 0.58	7.1×10^{-2}
$110^\circ < l < 220^\circ$	12	0.025	0.30	8	1.24 ± 0.60	1.9×10^{-2}
$220^\circ < l < 330^\circ$	23	0.015	0.45	19	0.96 ± 0.29	9.1×10^{-2}

^a Sources per square degree with $f_x > 0.1$ IPC counts s^{-1} .

All of these results are based on statistical analysis of the results of the Galactic Plane Survey. From these studies we have learned about the nature and distribution of low-flux galactic X-ray sources as a class. Studies of individual systems, both through optical identifications and X-ray analysis of selected sources, will further our understanding of galactic accretion sources.

We are grateful to the *Einstein* consortium teams at MIT and Columbia, as well as the guest observers G. Bignami and R. Lamb, for making their low-galactic latitude IPC observations available to us for inclusion in the Galactic Plane Survey. We also wish to thank F. R. Harnden, Jr., and D. Fabricant for help in developing the local detection algorithm, and the *Einstein* Data Aides for constant help in processing mountains of data.

REFERENCES

- Allen, C. W. 1973, *Astrophysical Quantities* (London: Athlone).
 Appaparo, K. M. V., et al. 1978, *Nature*, **273**, 450.
 Batten, A. H. 1967, *Pub. Dominion Ap. Obs.*, **8**, 119.
 Bignami, G. F., Caraveo, P. A., and Lamb, R. C. 1983, *Ap. J. (Letters)*, **271**, L9.
 Bignami, G. F., Caraveo, P. A., Lamb, R. C., Markert, T. H., and Paul, J. A. 1981, *Ap. J. (Letters)*, **247**, L85.
 Bradt, H. V. D., and McClintock, J. E. 1983, *Ann. Rev. Astr. Ap.*, **21**, 13.
 Chlebowski, T., Halpern, J. P., and Steiner, J. E. 1981, *Ap. J. (Letters)*, **247**, L35.
 Córdova, F. A., and Mason, K. O. 1983, in *Accretion Driven Stellar X-ray Sources*, ed. W. H. G. Lewin and P. J. v. d. Heuvel (Cambridge: Cambridge University Press), in press.
 Forman, W., Jones, C., Cominsky, L., Julien, P., Murray, S., Peters, G., Tananbaum, H., and Giacconi, R. 1978, *Ap. J. Suppl.*, **38**, 357.
 Giacconi, R. et al. 1978, "The HEAO B X-Ray Observatory Summary of Instrument Performance," CFA/HEA 78-214.
 Giacconi, R. et al. 1979a, *Ap. J.*, **230**, 540.
 Giacconi, R. et al. 1979b, *Ap. J. (Letters)*, **234**, L1.
 Gorenstein, P. 1975, *Ap. J.*, **198**, 95.
 Gottlieb, D. M. 1978, *Ap. J. Suppl.*, **38**, 287.
 Greenstein, J. L. 1974, *Ap. J. (Letters)*, **189**, L131.
 Griffiths, R. E., et al. 1983, *Ap. J.*, **269**, 375.
 Helfand, D. J., and Caillault, J.-P. 1982, *Ap. J.*, **253**, 760.
 Hertz, P. L. 1983, Ph.D. thesis, Harvard University.
 Hertz, P., and Grindlay, J. E. 1983a, *Ap. J. (Letters)*, **267**, L83.
 ———. 1983b, *Ap. J.*, **275**, 105.
 Hutchings, J. B., Crampton, D., and Cowley, A. P. 1981, *A.J.*, **86**, 871.
 Johnson, H. M. 1978, *Ap. J.*, **224**, 381.
 Komeseroff, M. M. 1965, *Australian J. Phys.*, **19**, 75.
 Lamb, R. C., and Markert, T. H. 1981, *Ap. J.*, **244**, 94.
 Lamb, R. C., Markert, T., Hartmann, R., Thompson, D., and Bignami, G. F. 1980, *Ap. J.*, **239**, 651.
 Landolt, A. 1973, *A.J.*, **78**, 959.
 Maccacaro, T. et al. 1982, *Ap. J.*, **253**, 504.
 Marshall, H. L. 1984, in preparation.
 Matilsky, T., Gursky, H., Kellogg, E., Tananbaum, H., Murray, S., and Giacconi, R. 1973, *Ap. J.*, **181**, 753.
 Matilsky, T. 1979, *Nature*, **280**, 298.
 McHardy, I. M., Lawrence, A., Pye, J. P., and Pounds, K. A. 1981, *M.N.R.A.S.*, **197**, 893.
 Murdoch, H. S., Crawford, D. F., and Jauncey, D. L. 1973, *Ap. J.*, **183**, 1.
 Patterson, J. 1983, *Ap. J. Suppl.*, submitted.
 Protheroe, R. J., and Wolfendale, A. W. 1980, *Astr. Ap.*, **84**, 128.
 Rappaport, S., and van den Heuvel, E. P. J. 1982, in *IAU Symposium 98, Be Stars*, ed. M. Jaschek and H. Groth (Dordrecht: Reidel), p. 327.
 Reid, C. A., Johnston, M. D., Bradt, H. V., Doxsey, R. E., Griffiths, R., and Schwartz, D. 1980, *A.J.*, **85**, 1062.
 Rosner, R., et al. 1981, *Ap. J. (Letters)*, **249**, L5.
 Rothenflug, R., Rocchia, R., and Casse, M. 1979, *Ap. J.*, **229**, 669.
 Smithsonian Astrophysical Observatory 1966, *SAO Star Catalogue* (Washington: Smithsonian Institution).
 Steiner, J. E., Ferrara, A., Garcia, M., Patterson, J., Schwartz, D. A., Warwick, R. S., Watson, M. G., and McClintock, J. E. 1983, *Ap. J.*, submitted.
 Steiner, J. E., Schwartz, D. A., Jablonski, F. J., Busko, I. C., Watson, M. G., Pye, J. P., and McHardy, I. M. 1981, *Ap. J. (Letters)*, **249**, L21.
 Stocke, J., et al. 1983, *Ap. J.*, **273**, 458.
 Topka, K., Avni, Y., Golub, L., Gorenstein, P., Harnden, F. R., Jr., Rosner, R., and Vaiana, G. S. 1982, *Ap. J.*, **259**, 677.
 Vaiana, G. S., et al. 1981, *Ap. J.*, **244**, 163.
 Wackerling, L. R. 1970, *Mem. R.A.S.*, **73**, 153.
 Walter, F. M. 1981, Ph.D. thesis, University of California (Berkeley).
 Warwick, R. S., et al. 1981, *M.N.R.A.S.*, **197**, 865.
 Watson, M. G., Willingale, R., Grindlay, J. E., and Hertz, P. 1981, *Ap. J.*, **250**, 142.
 White, N. E., Pravdo, S. H., Becker, R. H., Boldt, E. A., Holt, S. S., and Serlemitsos, P. J. 1980, *Ap. J.*, **239**, 655.
 Zombeck, M. V. 1980, SAO Special Report 386.

JONATHAN E. GRINDLAY: Harvard-Smithsonian Center for Astrophysics, 60 Garden Street, Cambridge, MA 02138

PAUL HERTZ: Naval Research Laboratory, Code 4121, Washington, DC 20375